Research Article

ENERGY EXPLORATION & EXPLOITATION

Energy Exploration & Exploitation
2020, Vol. 38(1) 298–309

DOI: 10.1177/0144598719877759
journals.sagepub.com/home/eea
SAGE

Investigation of the pyrolysis characteristics and kinetics of oil-palm solid waste by using Coats–Redfern method

Fredy Surahmanto[1], Harwin Saptoadi[2], Hary Sulistyo[3] and Tri A Rohmat[2]

Abstract

The pyrolysis kinetics of oil-palm solid waste was investigated by performing experiments on its individual components, including empty fruit bunch, fibre, shell, as well as the blends by using a simultaneous thermogravimetric analyser at a heating rate of 10°C/min under nitrogen atmosphere and setting up from initial temperature of 30°C to a final temperature of 550°C. The results revealed that the activation energy and frequency factor values of empty fruit bunch, fibre, and shell are 7.58–63.25 kJ/mol and 8.045E-02–4.054E + 04 s^{-1}, 10.45–50.76 kJ/mol and 3.639E-01–5.129E + 03 s^{-1}, 9.46–55.64 kJ/mol and 2.753E-01–9.268E + 03, respectively. Whereas, the corresponding values for empty fruit bunch–fibre, empty fruit bunch–shell, fibre–shell, empty fruit bunch–fibre–shell are 2.97–38.35 kJ/mol and 1.123E-02–1.326E + 02 s^{-1}, 7.95–40.12 kJ/mol and 9.26E-02–2.101E + 02 s^{-1}, 9.14–50.17 kJ/mol and 1.249E-01–2.25E + 03 s^{-1}, 8.35–45.69 kJ/mol and 1.344E + 01–4.23E + 05 s^{-1}, respectively. It was found that the activation energy and frequency factor values of the blends were dominantly due to the role of the components with a synergistic effect occurred during pyrolysis.

Keywords

Characteristics, Coats–Redfern, kinetics, oil-palm solid waste, pyrolysis

[1]Department of Mechanical Engineering Education, Universitas Negeri Yogyakarta, Yogyakarta, Indonesia
[2]Department of Mechanical and Industrial Engineering, Universitas Gadjah Mada, Yogyakarta, Indonesia
[3]Department of Chemical Engineering, Universitas Gadjah Mada, Yogyakarta, Indonesia

Corresponding author:
Fredy Surahmanto, Department of Mechanical Engineering Education, Universitas Negeri Yogyakarta, Yogyakarta, Indonesia.
Email: fredy_surahmanto@uny.ac.id

Introduction

Nowadays, renewable energy sources utilisation has been increasingly demanding due to the pressures on the global environment. Biomass is one of the most common forms that is widely used due to its abundant availability in agricultural and plantation residues. Currently, large scales of oil-palm (*Elaeis guineensis* Jacg.) plantations have been intentionally expanded for palm oil production in order to fulfil world's increasing palm oil demand. Consequently, the quantity of oil-palm solid waste, including empty fruit bunch (EFB), fibre, shell, and kernel will certainly be abundant. It can be quantitatively explained that for every ton of palm oil produced from fresh fruit bunches, approximately 1 t of EFB, 0.7 t of palm fibres, 0.3 t of palm kernels, and 0.3 t of palm shells remained (Chang, 2014). By this approximation, it can be estimated that for world's oil-palm production in 2017 as 66.86 million metric tons (USDA, 2017), the total biomass generated from the palm oil industry would be around 153.778 million metric tons. Hence, the oil-palm solid waste deserves appropriate concerns and handling for gaining great worth and minimising environmental impacts.

Due to the volume and environmental constraints, pyrolysis techniques have received much attention in recent years because they provide an attractive way to utilise waste. Recently, a number of investigations have been devoted on the pyrolysis characteristics and kinetic analysis of different rank coals blend with a variety of lignocellulosic biomass, including hazelnut shell (Haykiri-Acma and Yaman, 2010), giant reedgrass (Guan et al., 2015), plastic (Cai et al., 2008), printed circuit board scraps (Hao et al., 2014), corn stover and switchgrass (Bhagavatula et al., 2016), lignocellulosic components (Wu et al., 2014), and raw/torrefied wood (Lu et al., 2013). The findings of the above investigations revealed that pyrolysis is a promising, economic, and environmental-friendly technology for both energy production and waste handling. However, there is no report on the pyrolysis behaviours of both individual components and blends of oil-palm solid waste. Therefore, it is challenging to investigate the pyrolysis characteristics and kinetics of oil-palm solid waste, not only for their individual components but also their blends. The knowledge and understanding on kinetics of thermal decomposition of fuels or fuels blends is crucial to properly design and establish efficient conversion systems.

In this research, pyrolysis behaviours of both individual components and blends of oil-palm solid waste were investigated under inert atmosphere using a thermogravimetric (TG) analyser to obtain an overall understanding of their pyrolysis process. The Coats–Redfern method was applied to gain their kinetic parameters, for it had been successfully applied in the study of lignocellulosic waste (Fernandez et al., 2016).

Material and method

Material

Oil-palm solid waste, including EFB, fibre, and shell, used in this study were obtained from a palm oil mill in West Sumatra Province, Indonesia. Prior to experiments conducted, these materials were crushed into small particles and sieved into particles sized of 0.21 mm. Proximate, ultimate, and compositional analysis were done to these samples presented in Table 1.

Table 1. Proximate, ultimate, and compositional analysis of oil-palm solid waste.

Component	Empty fruit bunch	Fibre	Shell
Proximate analysis (wt%)			
Moisture content	8.503	7.736	7.630
Volatile matter	62.431	62.668	63.356
Fixed carbon	22.004	23.521	27.976
Ash	7.062	6.075	1.038
Higher heating value (cal/g)	3757.582	4359.673	4781.011
Ultimate analysis (wt%)			
Carbon	40.63	42.93	49.01
Hydrogen	6.11	6.09	6.18
Nitrogen	1.23	1.15	0.27
Sulphur	0.14	0.14	0.04
Oxygen	44.80	42.56	43.46
Compositional analysis (wt%)			
Hemicellulose	20.15	23.99	15.54
Cellulose	35.01	37.67	35.79
Lignin	19.65	22.99	36.96

TG experiment

An automatic simultaneous thermal analyser, which provides simultaneous TG and differential thermal analysis (DTA) on a single sample (Shimadzu, DTG-60, Japan, with temperature accuracy of 0.1 K, DTA sensitivity of 0.1 μV and TG sensitivity of 1 μg) was used to conduct pyrolysis tests. For every run, about 8 mg sample with particles size of 0.21 mm was used and 15 ml/min nitrogen was flowed to provide an inert atmosphere (Abu-Bakar and Moinuddin, 2012). Heating rate of 10°C/min, initial temperature of 30°C, and final temperature of 550°C were applied. The instrument provided continuous recording of TG and DTA curves and data that were used to calculate the kinetic parameters. Each experiment was repeated at least twice to ensure its reproducibility.

Kinetics theory

To perform the kinetic analysis of the reaction conversion curve, it is necessary to employ an integral analysis method. In the literature, different integral methods have been proposed for the determination of activation energy. The integral methods have been obtained from the corresponding approximations for the temperature integral, which does not have an exact analytical solution. Among these integral methods, the most commonly used in the kinetic analysis of thermal decomposition of coal and biomass is the integral method proposed by Coats and Redfern. The Coats and Redfern method for the determination of the activation energy has been extensively used in the kinetic analysis of thermal decomposition of coal, plastic, and biomass (Cai et al., 2008; Lu et al., 2013; Oyedun et al., 2014). Non-isothermal solid decomposition rate is mathematically expressed as (Ebrahimi-Kahrizsangi and Abbasi, 2008)

$$\frac{d\alpha}{dt} = kf(\alpha) \tag{1}$$

where α is flammable material conversion which is defined as

$$\alpha = \frac{m_i - m_t}{m_i - m_f} \tag{2}$$

k is the temperature dependent constant, expressed by Arrhenius equation as

$$k(T) = Ae^{\left(\frac{-E}{RT}\right)} \tag{3}$$

Function $f(\alpha)$ can be written as

$$f(\alpha) = (1-\alpha)^n \tag{4}$$

Substitution of equations (3) and (4) into equation (1) results in

$$\frac{d\alpha}{dt} = Ae^{-E/RT}(1-\alpha)^n \tag{5}$$

By using constant heating rate

$$\beta = \frac{dT}{dt} \tag{6}$$

Equation (5) can be arranged as

$$\frac{d\alpha}{dT} = \frac{A}{\beta}e^{-E/RT}(1-\alpha)^n \tag{7}$$

Solution of equation (7) results in

$$\ln\left[\frac{-ln(1-\alpha)}{T^2}\right] = \ln\left[\frac{AR}{\beta E}\left(1-\frac{2RT}{E}\right)\right] - \frac{E}{RT}; \quad \text{if } n = 1 \tag{8}$$

or

$$\ln\left[\frac{1-(1-\alpha)^{1-n}}{(1-n)T^2}\right] = \ln\left[\frac{AR}{\beta E}\left(1-\frac{2RT}{E}\right)\right] - \frac{E}{RT}; \quad \text{if } n \neq 1 \tag{9}$$

By using asymptotic approximation, where $2RT/E \ll 1$, so $ln\left[\frac{AR}{\beta E}\left(1-\frac{2RT}{E}\right)\right] \approx \left[\frac{AR}{\beta E}\right]$. Both plot $ln\left[\frac{-ln(1-\alpha)}{T^2}\right]$ versus $1/T$ for $n=1$ and plot $ln\left[\frac{1-(1-\alpha)^{1-n}}{(1-n)T^2}\right]$ versus $1/T$ for $n \neq 1$ will give linear curves. Activation energy, E and frequency factor, A can be determined by the slope and the intercept of the regression line.

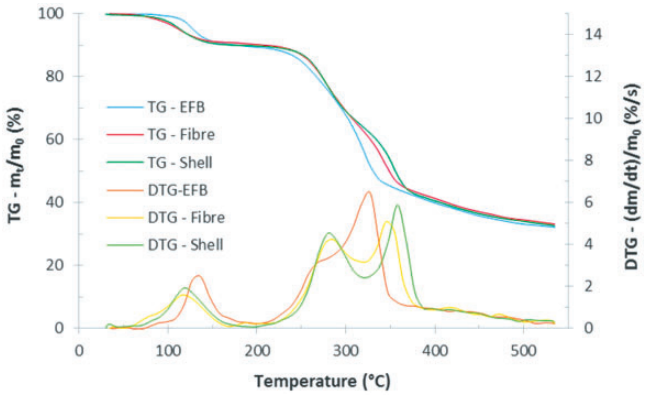

Figure 1. TG/DTG curves of EFB, fibre, and shell at a heating rate of 10°C/min. DTG: derivative thermogravimetric; EFB: empty fruit bunch; TG: thermogravimetric.

Results and discussion

Pyrolysis characteristics and kinetics of the components

Figure 1 shows the thermogravimetric (TG) and derivative thermogravimetric (DTG) curves of EFB, fibre, and shell, at a heating rate of 10°C/min. Pyrolysis process commonly comprises moisture evaporation, active pyrolysis (main devolatilisation), and passive pyrolysis (Fernandez et al., 2016). These stages also happened at EFB, fibre, and shell. As shown in Figure 1, EFB underwent moisture evaporation from initial temperature to 199°C with maximum mass loss rate of 2.45%/min at 137°C. This stage was also experienced by fibre and shell from initial temperature to 167 and 200°C with maximum loss rate of 1.6%/min at 116°C and 1.94%/min at 119°C, respectively.

Within the active pyrolysis stage in the DTG curves, two peaks of mass loss rate appear for fibre and shell. The first ones located on 286°C (4.24%/min) and 280°C (4.52%/min) while the later ones located on 345°C (5.09%/min) and 358°C (5.88%/min), for fibre and shell, respectively. It indicates that that hemicellulose and cellulose greatly took a rule in this stage. Meanwhile, only one mass loss peak appears in the devolatilisation of EFB, at about 328°C (6.44%/min) with a small shoulder located at the lower temperature side. This indicates that at least there was one major reaction scheme taking place during the pyrolysis process. The maximum peak of the DTG curve is probably contributed by the decomposition of the heavier fraction (cellulose) and the small shoulder corresponds to the lighter fraction (hemicellulose). The one peak of DTG data with small shoulder was also found for the pyrolysis of poplar wood as reported by Slopiecka et al. (2012).

As can be seen in Table 2, the values of activation energy and frequency factor for EFB vary from 7.58 to 63.25 kJ/mol and from 8.045E-02 to 4.054E + 04 s^{-1}, respectively. The lowest value of activation energy took place in the temperature range between 347 and 405°C, whereas the highest one took place in the temperature range between 308 and 327°C. Different from EFB, the values of activation energy and frequency factor for fibre, as can be seen in Table 2, vary from 10.45 to 50.76 kJ/mol and from 3.639E-01 to 5.129E + 03 s^{-1}, respectively. The lowest value of activation energy took place in the temperature range between 364 and 520°C, whereas the highest one took place in the

Table 2. The activation energy and frequency factor values of oil-palm solid waste components at different temperature ranges.

Samples	Temperature range (°C)	Activation energy (kJ/mol)	Frequency factor (s^{-1})	Coefficient of determination, R^2
EFB	228–248	17.03	4.55E-01	0.9714
	248–298	37.40	1.10E+02	0.9997
	308–327	63.25	4.05E+04	0.9987
	347–405	7.58	8.04E-02	0.9989
	425–535	12.63	3.20E-01	0.9913
Fibre	246–266	35.38	1.14E+02	0.9816
	266–285	50.76	5.13E+03	1.0000
	285–325	33.53	8.37E+01	0.9954
	325–364	49.15	2.74E+03	0.9927
	364–520	10.45	3.64E-01	0.9932
Shell	249–269	40.25	3.79E+02	0.9800
	269–289	52.81	8.21E+03	0.9973
	298–338	22.41	5.43E+00	0.9968
	338–377	55.64	9.27E+03	0.9934
	377–533	9.46	2.75E-01	0.9907

EFB: empty fruit bunch.

temperature range between 266 and 285°C. Being compared to fibre, shell has similar trend with fibre, where the activation energies and frequency factors for shell, as can be seen in Table 2, vary from 9.46 to 55.64 kJ/mol and from 2.753E-01 to 9.268E + 03 s^{-1}, respectively. The lowest value of activation energy took place in the temperature range between 377 and 533°C, whereas the highest one took place in the temperature range between 338 and 377°C.

Based on the compositional analysis, these three components of oil-palm solid waste are mainly constituted of hemicellulose, cellulose, and lignin. As presented in Table 1, the proportions of cellulose, hemicellulose, and lignin in the shell are 15.54, 35.79, and 36.96 wt%, respectively, indicating that the lignin contents are high and the cellulose contents are low. Inversely, the cellulose contents are high and lignin contents are low in EFB and fibre. In more detail, the proportions of those constituents in EFB are 20.15, 35.01, and 19.65 wt%, whereas the corresponding contents in the fibre are 23.99, 37.67, and 22.99 wt%. These composition analysis results are similar with the previous studies (Shibata et al., 2008). Hemicellulose and cellulose are highly reactive and completely pyrogenic in the temperature range of 200–400°C, while lignin decomposes at lower rate in a broader temperature range. Therefore, the second stage was dominantly generated by the decomposition of hemicellulose and part of lignin. The third stage reflected the decomposition of cellulose and remaining lignin. This would appear to indicate that the curves of EFB, fibre, and shell are greatly influenced by the amount of cellulose, hemicellulose, and lignin in each (Orfao et al., 1999). So the pyrolysis process of them was essentially the thermal decompositions of the three constituents.

Pyrolysis characteristics and kinetics of the blends

Figure 2 shows the TG and DTG curves of equal proportion–blends: EFB–fibre (50%–50%), EFB–shell (50%–50%), fibre–shell (50%–50%), and EFB–fibre–shell

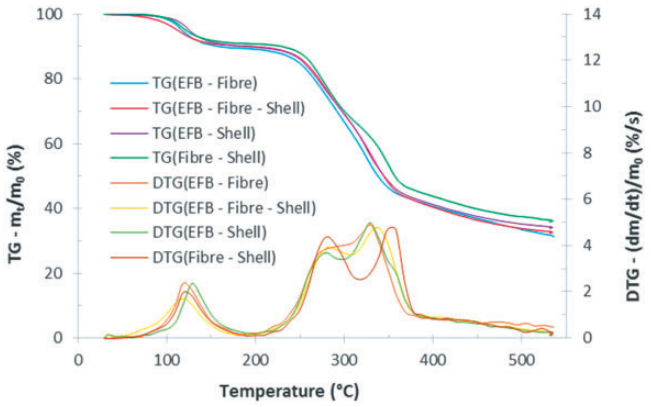

Figure 2. TG/DTG curves of blends at a heating rate of 10°C/min. DTG: derivative thermogravimetric; EFB: empty fruit bunch; TG: thermogravimetric.

(33.33%–33.33%–33%) at a heating rate of 10°C/min. It can be seen that the influence of the high cellulose content in EFB and fibre as well as the high lignin content in shell plays a significant role in the thermal decomposition process on their blends.

In more detail, it appears in Figure 3(a) that the DTG curve of EFB–fibre blend has a similar shape as that of EFB, in which both have only one mass loss peak appearing in the devolatilisation of EFB, with a small shoulder located at the lower temperature side. This may be due to the influence of high cellulose content in EFB and fibre. On the contrary, the DTG curve of EFB–shell blend, as shown by Figure 3(b), could not form only one mass loss peak with a small shoulder, anymore, because of the significant involvement of lignin content in shell. Likewise, two mass loss peaks are found in Figure 3(c) and (d), even though it can be observed that the valley of the EFB–fibre–shell blend is shallower than that of fibre–shell blend, due to the mixing role of the three constituents. Overall, it can be seen in Figure 3(a) to (d) that the curves of all blends with equal component composition are nearly the mean of the mass loss rate of its components. However, the curves of the experimental blends and the theoretical ones are nearly coincident.

To further investigate the synergistic effect among the oil-palm solid waste, the difference of weight loss, $\Delta W = W_{\text{blend}} - \sum_{i=1}^{n}(x_i.W_i)$, was calculated. Obviously, ΔW describes the extent of synergistic effect during the pyrolysis of these blends. Figure 4 shows the variation of ΔW with temperature for the blends of oil-palm solid waste components. It can be observed that in the moisture evaporation and active pyrolysis stage, ΔW curves for EFB–fibre blend, EFB–shell blend, and fibre–shell blend have similar trends, whereas ΔW curve for EFB–fibre–shell blend shows different trend from the others, where it did not have minimum value in the moisture evaporation stage. Then, in the passive pyrolysis stage, ΔW slightly decreases for EFB–shell blend and fibre–shell blend, but it increases for EFB–fibre blend and nearly stable for EFB–fibre–shell blend. The maximum and minimum ΔW values for all blends are presented in Table 3. At the devolatilisation stage, the ΔW (from −3.25 to −4.86%) of the four blends indicates that a synergistic effect occurred during pyrolysis.

Furthermore, it has been known from previous research findings that cellulose, hemicellulose, and lignin decomposed at different temperature ranges (Dorez et al., 2014). It was

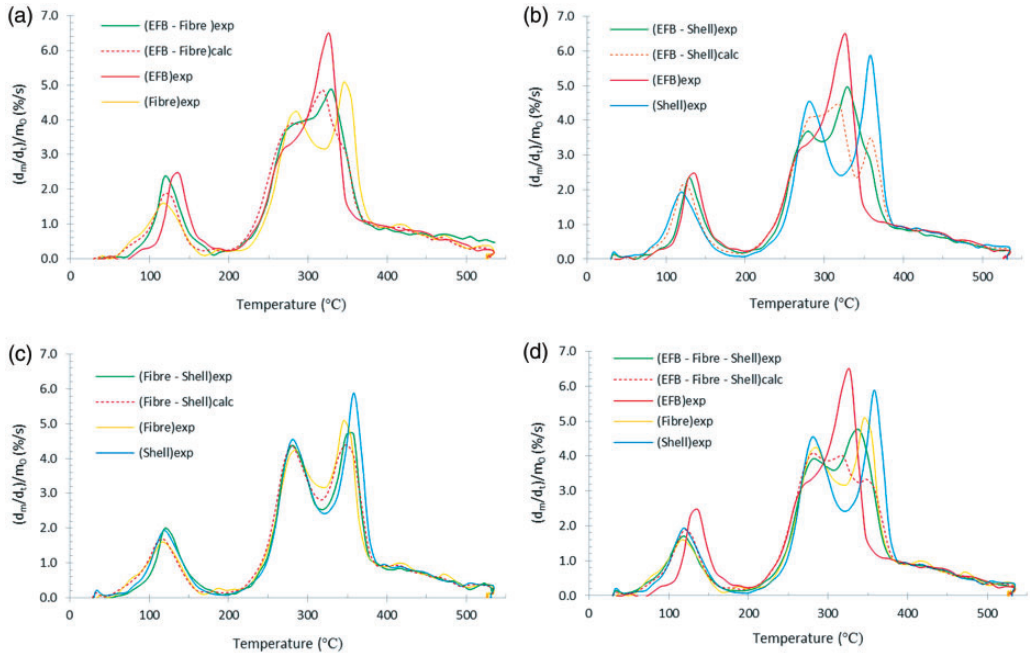

Figure 3. Comparison of DTG curves of blends with their components at a heating rate of 10°C/min. (a) Blend of EFB–fibre, (b) blend of EFB–shell, (c) blend of fibre–shell, and (d) blend of EFB–fibre–shell. EFB: empty fruit bunch.

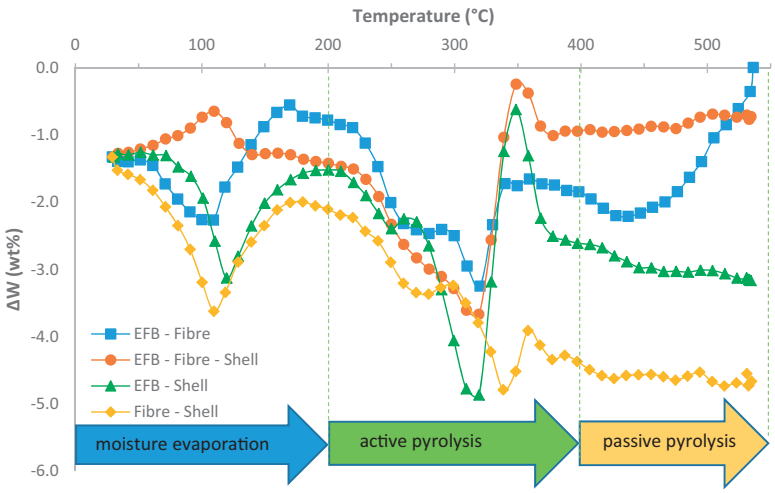

Figure 4. Variation of ΔW for the oil-palm solid waste blends. EFB: empty fruit bunch.

found that lignin started to decompose at low rate and low temperature of about 200°C and continued until 600°C. Thus, it decomposed at both active and passive pyrolysis stage, whereas hemicellulose decomposed between 200 and 350°C. Then, cellulose is the last component that decomposed at higher temperature range of 280–400°C. By considering the

Table 3. The maximum and minimum ΔW values for all mixtures.

Mixture	$\Delta W_{min,1}$ (%)	$T_{min,1}$ (°C)	$\Delta W_{max,1}$ (%)	$T_{max,1}$ (°C)	$\Delta W_{min,2}$ (%)	$T_{min,2}$ (°C)	$\Delta W_{max,2}$ (%)	$T_{max,2}$ (°C)
EFB–fibre	−2.27	109.32	−0.56	169.64	−3.25	320.18	−1.66	359.33
EFB–shell	−3.13	119.65	−1.52	200.23	−4.86	319.36	−0.62	348.61
Fibre–shell	−3.62	109.56	−1.99	179.94	−4.79	338.52	−3.90	358.07
EFB–fibre–shell	–	–	−0.65	109.75	−3.67	319.24	−0.25	348.75

EFB: empty fruit bunch.

decomposition temperature ranges of those three components, two peaks of the DTG curves in both active and passive pyrolysis stage for the blends in Figure 3 can be related to the decomposition of hemicellulose, cellulose, and lignin. The first peak probably involved hemicellulose and lignin decomposition, while the second peak was formed of cellulose and lignin decomposition. Cellulose is a semi-crystalline material, while lignin and hemicellulose are non-crystalline so the pyrolysis of cellulose must first destroy the lattice of crystals that needs energy, leading to higher activation energy (Mae et al., 2000).

As can be seen in Table 4, the activation energy and frequency factor values for blend of EFB–fibre vary from 2.97 to 38.35 kJ/mol and from 1.123E-02 to 1.326E + 02 s^{-1}, respectively. The lowest value of activation energy took place in the temperature range between 359 and 417°C, whereas the highest one took place in the temperature range between 249 and 269°C. Still in the second temperature range, about 249–349°C, EFB–fibre blend had the high activation energy values, but then it had the low activation energy in the three higher temperature ranges, about 359–533°C. This could be possibly caused by the role of high content of cellulose in both EFB and fibre.

Different from the blend of EFB–fibre, the activation energies and frequency factors for blend of EFB–shell vary from 7.95 to 40.12 kJ/mol and from 9.260E-02 to 2.101E + 02 s^{-1}, respectively. The lowest value of activation energy took place in the temperature range between 368 and 387°C, whereas the highest one took place in the temperature range between 259 and 358°C.

Meanwhile, fibre–shell blend had high activation energy in its second, third, and fourth temperature ranges. The activation energy and frequency factor values for fibre–shell blend vary from 9.14 to 50.17 kJ/mol and from 1.249E-01 to 2.250E + 03 s^{-1}, respectively. The lowest value of activation energy took place in the temperature range between 367 and 532°C, whereas the highest one took place in the temperature range between 249 and 289°C.

Lastly, the activation energies and frequency factors for blend of EFB–fibre–shell vary from 8.35 to 45.69 kJ/mol and from 1.344E + 01 to 4.230E + 05 s^{-1}, respectively. The lowest value of activation energy took place in the temperature range between 210 and 240°C, whereas the highest one took place in the temperature range between 249 and 358°C.

It is obvious that every blend has its own temperature ranges with nearly the same range. In addition, the activation energy and frequency factor values of the blends are different from those of each component. This ensures that the pyrolysis mechanism of blends is different from that of each component.

It needs to be noted that the coefficient of determination (R^2) is employed to obtain the activation energy in various methods. When applying Coats–Redfern method, the coefficient of determination is a measure of how well the regression line represents the data and

Table 4. The activation energy and frequency factor values of (a) EFB–fibre, (b) EFB–shell, (c) fibre–shell, and (d) EFB–fibre–shell at different temperature ranges.

Samples	Temperature range (°C)	Activation energy (kJ/mol)	Frequency factor (s^{-1})	Coefficient of determination, R^2
EFB–fibre (50%–50%)	249–269	38.35	1.33E+02	0.9976
	269–349	37.97	1.22E+02	0.9989
	359–417	2.97	1.12E-02	0.9875
	427–466	3.39	1.37E-02	0.9940
	476–533	6.18	3.91E-02	0.9947
EFB–shell (50%–50%)	229–250	15.79	3.04E-01	0.9456
	259–358	40.12	2.10E+02	0.9982
	368–387	7.95	9.26E-02	0.9863
	397–436	8.33	1.04E-01	0.9987
	445–533	10.13	1.70E-01	0.9989
Fibre–shell (50%–50%)	229–249	12.66	1.04E-01	0.9665
	249–289	50.17	2.25E+03	0.9941
	289–328	26.49	7.67E+00	0.9905
	328–367	46.73	7.58E+02	0.9905
	367–532	9.14	1.25E-01	0.9953
EFB–fibre–shell (33.33%–33.33%–33.33%)	210–240	8.35	1.34E+01	0.9396
	249–358	45.69	4.23E+05	0.9991
	368–407	13.30	2.64E+02	0.9999
	416–475	16.37	5.57E+02	0.9999
	484–533	19.48	1.09E+03	0.9997

EFB: empty fruit bunch.

reflects the validity of the obtained activation energy for the method. It is clear that the obtained activation energy and coefficient of determination for the reactions from the Coats–Redfern method is substantially determined by the selection of temperature regions corresponding to the main mass loss stages varied with the heating rate. The different ranges of temperature were results of selecting adjacent points (in the plot $\ln\left(-\ln(1-\alpha)/T^2\right)$ versus $1/T$ that could be approximated by line segments with the best coefficient of determination (R^2). This selection can describe four and five consecutive first-order reactions in the pyrolysis of the oil-palm solid waste.

Conclusions

Summing up the results, it can be concluded that the curves of EFB, fibre, and shell were influenced by the content of cellulose, hemicellulose, and lignin. So, the pyrolysis process of them was essentially the thermal decompositions of these three constituents. The curves of all blends with equal component composition reflect nearly the average value of the mass loss rate of its components. Moreover, the curves of the experimental blends and the theoretical ones are nearly coincident. This would seem to suggest that the activation energy and frequency factor values of the blends were dominantly due to the role of the components with a synergistic effect (ΔW values ranges from -3.25 to -4.86%) occurred during pyrolysis.

The Coats–Redfern method has been successfully applied to determine the kinetic parameters, including activation energy and frequency factor, of the pyrolysis oil-palm solid waste by selecting the adjacent points in the plot of $ln\left(-\ln(1-\alpha)/T^2\right)$ versus $1/T$ which could be approximated as line segments that have best coefficient of determination (R^2).

Declaration of conflicting interests

The author(s) declared no potential conflicts of interest with respect to the research, authorship, and/or publication of this article.

Funding

The author(s) received no financial support for the research, authorship, and/or publication of this article.

ORCID iD

Fredy Surahmanto https://orcid.org/0000-0002-2148-1152

References

Abu-Bakar AS and Moinuddin KAM (2012) Effects of variation in heating rate, sample mass and nitrogen flow on chemical kinetics for pyrolysis. In: *Proceedings of the 18th Australasian fluid mechanics conference*, Launceston, Australia, 3-7 December 2012, pp.18–21. Launceston: Australasian Fluids Mechanics Society.

Bhagavatula A, Shah N and Honaker R (2016) Estimating the pyrolysis kinetic parameters of coal, biomass, and their blends: a comparative study. *Energy & Fuels* 30: 10045–10054.

Cai J, Wang Y, Zhou L, et al. (2008) Thermogravimetric analysis and kinetics of coal/plastic blends during co-pyrolysis in nitrogen atmosphere. *Fuel Processing Technology* 89: 21–27.

Chang SH (2014) An overview of empty fruit bunch from oil palm as feedstock for bio-oil production. *Biomass and Bioenergy* 62: 174–181.

Dorez G, Ferry L, Sonnier R, et al. (2014) Effect of cellulose, hemicellulose and lignin contents on pyrolysis and combustion of natural fibers. *Journal of Analytical and Applied Pyrolysis* 107: 323–331.

Ebrahimi-Kahrizsangi R and Abbasi MH (2008) Evaluation of reliability of Coats-Redfern method for kinetic analysis of non-isothermal TGA. *Transactions of Nonferrous Metals Society of China* 18: 217–221.

Fernandez A, Saffe A, Pereyra R, et al. (2016) Kinetic study of regional agro-industrial wastes pyrolysis using non-isothermal TGA analysis. *Applied Thermal Engineering* 106: 1157–1164.

Guan Y, Ma Y, Zhang K, et al. (2015) Co-pyrolysis behaviors of energy grass and lignite. *Energy Conversion and Management* 93: 132–140.

Hao J, Wang H, Chen S, et al. (2014) Pyrolysis characteristics of the mixture of printed circuit board scraps and coal powder. *Waste Management* 34(10): 1763–1769.

Haykiri-Acma H and Yaman S (2010) Interaction between biomass and different rank coals during co-pyrolysis. *Renewable Energy* 35: 288–292.

Lu K-M, Lee W-J, Chen W-H, et al. (2013) Thermogravimetric analysis and kinetics of co-pyrolysis of raw/torrefied wood and coal blends. *Applied Energy* 105: 57–65.

Mae K, Hasegawa I, Sakai N, et al. (2000) A new conversion method for recovering valuable chemicals from oil palm shell wastes utilizing liquid-phase oxidation with H_2O_2 under mild conditions. *Energy & Fuels* 14: 1212–1218.

Orfao J, Antunes FJA and Figueiredo JL (1999) Pyrolysis kinetics of lignocellulosic materials-three independent reactions model. *Fuel* 78: 349–358.

Oyedun AO, Tee CZ, Hanson S, et al. (2014) Thermogravimetric analysis of the pyrolysis characteristics and kinetics of plastics and biomass blends. *Fuel Processing Technology* 128: 471–481.
Shibata M, Varman M, Tono Y, et al. (2008) Characterization in chemical composition of the oil palm (*Elaeis guineensis*). *Journal of the Japan Institute of Energy* 87(5): 383–388.
Slopiecka K, Bartocci P and Fantozzi F (2012) Thermogravimetric analysis and kinetic study of poplar wood pyrolysis. *Applied Energy* 97: 491–497.
USDA (2017) *World's Palm Oil Production*. Washington, DC: USDA.
Wu Z, Wang S, Zhao J, et al. (2014) Synergistic effect on thermal behavior during co-pyrolysis of lignocellulosic biomass model components blend with bituminous coal. *Bioresource Technology* 169: 220–228.

Appendix

Notation

A	frequency factor (s^{-1})
E	activation energy (kJ/mol)
k	temperature dependent constant
m_f	final mass (kg)
m_i	initial mass (kg)
m_t	mass at time t (kg)
n	reaction order
R	universal gas constant, 8.314 J/(mol K)
T	temperature (°C)
W_{blend}	weight loss of blend (kg)
W_i	weight loss of each material (kg)
x_i	weight fraction of each material
α	material conversion
β	heating rate (°C/min)
ΔW	weight loss difference